Polylactide/Clay Nanocomposites: A Fresh Look into the *In Situ* Polymerization Process

Alexandre Carneiro Silvino, Kenia Santos de Souza, Karim Dahmouche, Marcos Lopes Dias

Instituto de Macromoléculas Professora Eloisa Mano, Universidade Federal do Rio de Janeiro, CT, Bloco J, Ilha do Fundão, Rio de Janeiro, RJ, Brazil

Received 29 April 2011; accepted 20 June 2011
DOI 10.1002/app.35120
Published online 12 October 2011 in Wiley Online Library (wileyonlinelibrary.com).

ABSTRACT: Polylactide nanocomposites with organo-modified montmorillonite presenting a high degree of clay exfoliation were prepared via *in situ* polymerization by using an improved methodology. The morphology of the nanocomposites was studied by WAXD and SAXS. The size distribution of clay aggregates in the polylactide matrices was quantitatively determined by SAXS applying the stacked-disk model. The analyses show high degree of delamination of the silicate yielding exfoliated polylactide nanocomposites even at high concentration of clay (>10 wt %). L-lactide conversions measured by ATR-FTIR were determined to be no less than 94% after 3 h of reaction in all polymerizations. DSC measurements were performed to study the influence of the clay content on the thermal behavior of the prepared nanocomposites. © 2011 Wiley Periodicals, Inc. J Appl Polym Sci 124: 1217–1224, 2012

Key words: polylactide; nanocomposite; SAXS; clay; *in situ* polymerization

INTRODUCTION

In recent years, polylactide (PLA) have received intensive attention due to its biodegradability and biocompatibility properties. PLA is an aliphatic polyester produced from renewable resources that finds many applications in medicine, fiber technology, and packaging.[1] Nevertheless, to render PLA able to compete with commodity polymers and expand its end-use applications, properties such as thermal stability and gas permeability still needed to be improved. The incorporation of layered silicates into the polymer matrix has been studied extensively as a strategy for improvements in HDT (heat distortion temperature), dynamic mechanical, flexural, and barrier properties of innumerous polymers including polylactide and other polyesters.[2] Several approaches have been considered to prepare PLA/layered silicate nanocomposites. Among them all, the *in situ* polymerization has been claimed as the most efficient method for obtaining high degree of clay exfoliation into the polylactide matrix.[3] Some results previously reported in the literature suggest that the highest properties improvements can only be achieved when the silicate is fully exfoliated in the polymer matrix.[4] However, compared with other techniques, the *in situ* polymerization is not an attractive technique from an industrial point of view. As a consequence, few papers have addressed it as a method to prepare PLA nanocomposites.[5] On the other hand, it is relevant to mention that intercalative *in situ* polymerization can be considered as a strategy to prepare masterbatches, i.e., polymer nanocomposites with high content of delaminated clay (up to 50 wt %) that can be dispersed into pure polymer matrix to achieve a final clay content of 2 to 5 wt %. In a previous study reported by Paul et al., exfoliated polylactide nanocomposites were prepared in bulk by using tin(II) 2-ethyl-hexanoate [$Sn(Oct)_2$] and triethylaluminum in the presence of an organo-modified montmorillonite with an intercalant containing hydroxyl groups (Cloisite® 30B).[6] Although that strategy may produce exfoliated polylactide/clay nanocomposites, the reaction times (12 h or more) can be considered too long for industrial purposes and the size distribution of the clay aggregates in the polylactide matrix was not investigated quantitatively. In this work we describe the preparation and characterization of PLA/montmorillonite nanocomposites with high degree of clay exfoliation and the quantitative determination of the size distribution of the clay fragments by small angle X-ray scattering. The catalytic system was prepared by employing a different approach to fix tin centers in the organo-modified montmorillonite and its performance was monitored by quantitative ATR-FTIR

Correspondence to: A. C. Silvino (alexandresilvino@ima.ufrj.br).

Contract grant sponsors: Conselho Nacional de Desenvolvimento Científico e Tecnológico (CNPq), Coordenação de Aperfeiçoamento de Pessoal de Nível Superior (CAPES), the Brazilian Synchrotron Light Laboratory (LNLS, Campinas - Brazil).

technique. Parameters such as tin content and structure of the catalytic system were studied and the morphologies of the resulting PLA/organo-modified nanocomposites were investigated. The thermal behavior of the nanocomposites was also investigated in relation of the clay content of the organo-modified montmorillonite.

EXPERIMENTAL

Materials

All experiments were carried out under purified nitrogen using standard Schlenk techniques or in a glove-bag. Toluene and heptane were distilled from Na/benzophenone under nitrogen. The L,L-Lactide was purchased from Boehringer Ingelheim and used without any purification (the free acid content measured by potentiometric titration was < 1 meq/kg). The organo-modified montmorillonite (Cloisite® 30B) was supplied by Southern Clay Products and was dried under vacuum at 70°C for 24 h before use. Tin(II) 2-ethy-hexanoate was purchased from Aldrich and used as received.

Preparation of the catalyst

In a Schlenk flask, 5.0 g of the organo-modified montmorillonite (Cloisite® 30B) were treated with 10.0 mL of Tin(II) 2-Ethyl-hexanoate in presence of 10 mL de heptane at 75°C. After 4 h of vigorous stirring, the product was washed with 60 mL of toluene and dried under reduced pressure. A solid catalyst powder was obtained. The content of tin of the catalyst powder was determined to be 9.8% by atomic absorption spectrophotometry.

Polymerizations (typical procedure)

In glove-bag 0.31 g of the catalyst and 8.25 g of L,L-lactide were transferred to a glass ampoule previously dried in oven at 100°C for 24 h. The ampoule containing the catalyst and the monomer was sealed and placed in an oil bath at 160°C and the polymerization was carried out for 3 h. After the reaction time, the ampoule was cooled down to room temperature and then broken. Its contents were exposed to air and taken for analyses.

Characterization and measurements

The content of tin of the catalyst was determined using a Shimadzu AA 6800 atomic absorption spectrophotometer. The instrument settings were kept constant (8 mA lamp, aperture 1.0 nm, wavelength $\lambda = 286.3$ nm, gas flow = 1.8 L/min, Acetylene flame). The sample was prepared using silicate decomposition as follows: 0.0623 g of the catalyst was weighed and placed into a PTFE vessel (made of Teflon®) in which 0.5 mL of aqua regia (1 : 3 HNO_3/HCl) + 3 mL of HF + 40 mL of deionized water + 2.8 g of H_3BO_3 were added. The mixture was stirred until complete dissolution of the sample. Then the solution was transferred to a volumetric flask and the volume completed to 100 mL.

The organo-modified montmorillonite (Cloisite® 30B) and the catalyst spectra were acquired using ATR-FTIR (Attenuated Total Reflectance—Fourier Transform Infrared) under nitrogen. For polymer conversion analyses, films of the samples (polylactide/lactide) were cast onto KBr pellets (IR grade from Sigma Aldrich) from chloroform solutions (concentration of 0.1 g/mL) and the solvent was allowed to evaporate prior to measurement. No evidence of residual solvent was observed spectroscopically. All spectra were recorded on an Excalibur 3100 FTIR in the range of 4000–400 cm^{-1} (100 scans, 4 cm^{-1} resolution). Absorption peak areas at 1454 and 935 cm^{-1} of the films spectra were determined using the software package Revolution Pro (Varian®) according to the baseline method.[7] In this method, a straight line was established between two fixed points on the spectra insensitive to composition located at wavenumbers below and above the peaks of interest. A calibration curve with well-defined mixtures of lactide and PLA was built according to the method established by Braun et al. using the reference peaks at 1454 and 935 cm^{-1}.[8] The absolute concentration dependence of the absorption was eliminated by normalizing the intensity at the characteristic wavelength for one component by a signal at a wavelength shared by both compounds (1454 cm^{-1}). The conversions of the samples were calculated using the linear fit of the inverse of conversion of the defined mixtures of PLA/lactide as a function of the peak area ratio (special case III—lactide concentration of 10 wt % or less).

Wide Angle X-ray Diffraction (WAXD) analyses were performed in a Rigaku Miniflex (model DMAX 2200) X-ray diffractometer (generator of 3 kW, a graphite monochromator, CuK_α radiation (wavelength, $\lambda = 0.154$ nm), operated at 30 kV/15 mA. The samples were scanned with a counting time of 1 s under a diffraction angle of 2θ in the range of 2.0 to 40.0°.

The glass transition (T_g), the melting temperature (T_m), the crystallization temperature on heating (T_{hc}), and the crystallization temperature on cooling (T_{cc}) of the nanocomposites were determined using a DSC-7 calorimeter (Perkin–Elmer Inc., Wellesley, MA) with a heating and cooling ramp of 20°C/min from 25 to 200°C under nitrogen flow and the values were recorded during the second scans. The degree of crystallinity (X_c) of samples was calculated

considering the melting enthalpy of 100% crystalline poly(L-lactide) as 106 J/g.[9,10]

The small angle X-ray scattering experiments were carried out at the SAXS01 beam line of the Brazilian Synchrotron Light Laboratory (LNLS), Campinas (Brazil) with a fixed wavelength of 1.608 Å under vacuum at room temperature. The scattering intensity $I(q)$ was plotted as a function of the wave vector $q = 4\pi\sin\theta/\lambda$, where θ is the scattering angle. The scattering intensity was normalized by subtracting the background scattering and taking account of the sample thickness.

RESULTS AND DISCUSSION

Catalyst preparation and characterization

As mentioned before, in Paul et al.'s study, exfoliated PLA/clay nanocomposites were prepared in bulk by using a tin carboxilate in the presence of an organo-modified montmorillonite (Cloisite® 30B). In contrast, they also reported that when polymerizations were carried out in presence of Cloisite® 25A, an organo-modified clay with no hydroxyl groups in the organophilization agent, the product is invariably, an intercalated polymer. These results suggest the formation of alkoxide active species involving the metal and the hydroxyl groups inside the clay. After 1 h of clay swelling, the molten monomer subsequently penetrates the silicate galleries to react with the tin centers anchored on the hydroxyl groups in the Cloisite® 30B. To make sure the polymerization centers are fixed within the clay galleries, we decided to treat the clay with $Sn(Oct)_2$ before reaction and wash the product with toluene to remove any tin center from the clay surface thus enhancing the delamination efficiency.

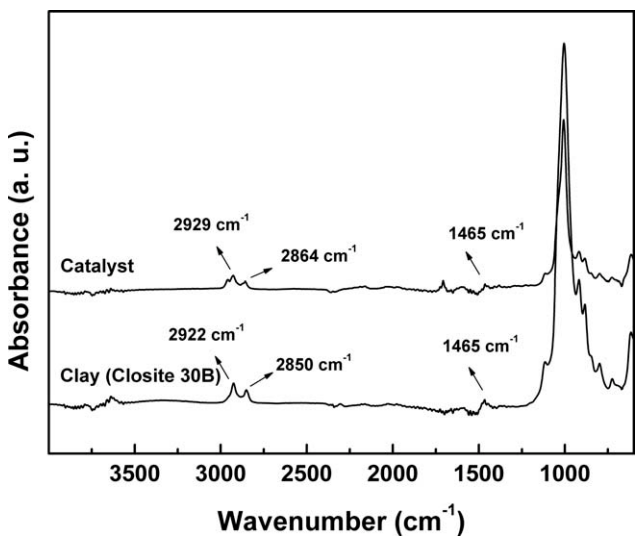

Figure 1 FTIR spectra of the clay (Cloisite® 30B) and the catalyst.

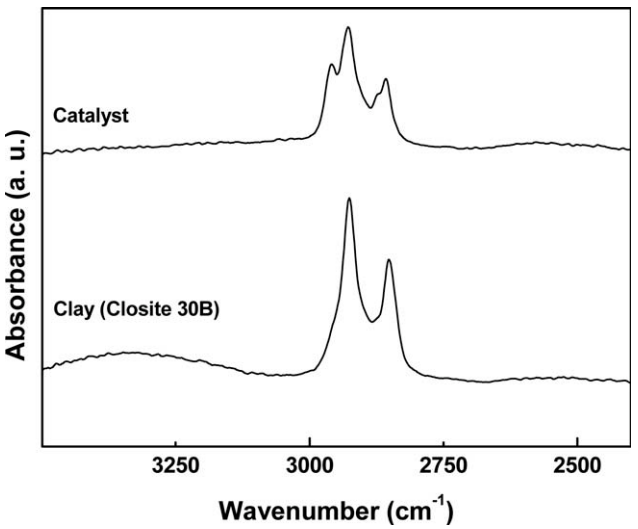

Figure 2 FTIR spectra of the clay (Cloisite® 30B) and the catalyst (region between 3500 and 2400 cm^{-1}).

The infrared spectra of the organo-modified clay and catalyst were carried out in the area 4000–600 cm^{-1} (Figs. 1 and 2). A broad signal at 3339 cm^{-1} in the spectrum of the pure clay can be assigned to the O—H stretching mode of the hydroxyl groups in the organophilic filler.[11] That signal does not appear in the catalyst spectrum, suggesting the formation of tin-alkoxide species. The signals at 2924 cm^{-1} and 2850 cm^{-1} in the clay spectrum are due to the stretching vibration of the alkyl C—H bonds of the hydroxyethyl, methyl and tallowalkyl groups and they agree with values reported in the literature.[12,13] Those vibrations are also present in the treated clay, however weak signals at 2958 cm^{-1} and 2872 cm^{-1} in the spectrum of the organo-modified clay treated with tin(II) 2-ethyl-hexanoate indicate more than one type of C—H stretching in the catalyst. The intense signal at 1007 cm^{-1} present in both spectra can be assigned to the Si—O stretching of the silicate.[14,15]

Nanocomposites structure

The structure of the nanocomposites was investigated by Wide Angle X-ray Diffraction (WAXD). Figure 3 represents the patterns of the pure Cloisite® 30B powder and the PLA/clay nanocomposites in the range of $2\theta = 2$–40^o. The WAXD results suggest high degree of clay exfoliation in the polylactide matrix through the absence of the diffraction peak characteristic of the organo-modified silicate at low 2θ angles (Cloisite® 30B d-spacing = 18.4 Å).[16] The disappearance of the basal peak suggests the formation of an exfoliated structure.

To confirm quantitatively the suggested very good dispersion of clay in the polymer, SAXS experiments were performed. A detailed discussion of the scattering theory of layers and plates can be found in the

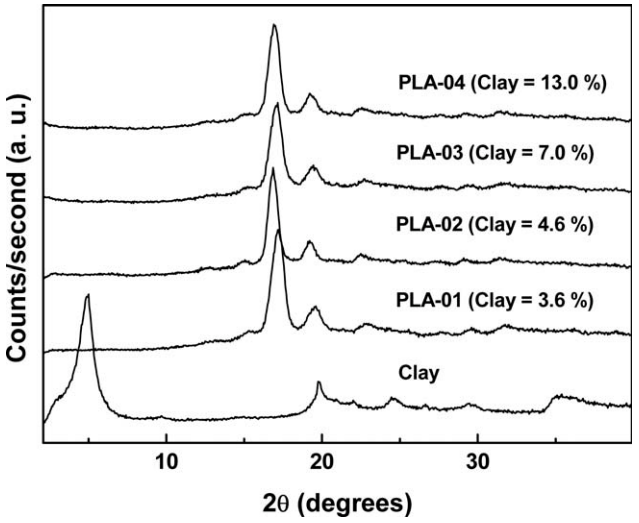

Figure 3 WAXD patterns for the organo-modified montmorillonite and the PLA/clay nanocomposites.

literature.[17] In this work the stacked-disc model was used to determine quantitatively the fraction of clay aggregates (tactoids) of thickness t dispersed in the polymer.[18] The aspect ratio of the plate was used and we have considered a wide distribution of tactoid thicknesses. In the case of flat particles of thickness t, the small angle intensity is given by the following law:

$$P(q) = \frac{B}{q^2}\Delta\rho^2 t^2 \left(\frac{\sin(qt/2)}{qt/2}\right)^2 \quad (1)$$

where B is a constant proportional to developed surface of the particle and $\Delta\rho$ is the difference between electronic densities of the matrix and the filler (clay).[17] A distribution of thickness was assumed and the spectrum was considered as being the sum of contributions of several populations, a fixed number of platelets in a stack constituting a population. The weighted sum of the contributions arising from entities of thickness t_i is then:

$$P(q) = \sum_{i=1}^{n} \frac{B_i}{q^2} t_i^2 \left(\frac{\sin(qt_i/2)}{qt_i/2}\right)^2 \quad (2)$$

The proportion P_i of the tactoids of size t_i within the matrix can be estimated with the relation:

$$P_i = \frac{B_i}{\sum_j B_j} \quad (3)$$

It is important to note that the stacked-disc model does not take into account the interactions between different clay tactoids or platelets which may become more significant for greater clay loadings. In attempt to account for the possible correlation bump originating from interparticle correlations observed in the nanocomposites spectra, the following structure factor (well-known for not too anisometric nano-objects presenting spatial correlation[19]) was used:

$$S(q) = \frac{1}{1 + k\omega(q)} \quad (4)$$

$$\omega(q) = 3\frac{(\sin qd) - qd\cos(qd)}{(qd)^3} \quad (5)$$

Two new parameters are introduced: the characteristic distance d between tactoids (d is thus a correlation length and can be seen as a pseudo spatial-periodicity) and the packing factor k related to the magnitude of correlation effects.[19,20] The theoretical SAXS intensity $I(q)$ is then the product

$$P(q)S(q) \quad (6)$$

A least square fitting procedure was applied to fit the experimental SAXS curves with eq. (6). For all samples, the best fit of SAXS intensity was performed up to 0.130 $Å^{-1}$. The good agreement between both the theoretical equation and experimental curves (Fig. 4) allowed to determine the parameters B_i and t_i. Note that, for all samples, the best fit was obtained by using only three families of clay aggregates, having thickness t_1, t_2, and t_3. The range of the values of t_1, t_2, and t_3 is presented in Table I for each nanocomposite.

The populations of the clay aggregates in the polylactide matrices calculated employing this procedure showed that the proportion of aggregates with thickness around 20 Å or less was greater than 99% for all nanocomposites (Table I). These results agree with the absence of the basal peak of the organo-modified clay previously discussed in the wide angle X-ray diffraction patterns and confirm that the tin catalyst can be used to prepare PLA/clay nanocomposites with high degree of exfoliation even with high clay loadings (13 wt %). According to the fraction of bigger aggregates determined for all samples the content of intact clay tactoids is very low and does not have strong influence in the SAXS curve shape, however, interactions between the

TABLE I
Area Fraction of Thickness t in the PLA/Clay Nanocomposites Obtained from SAXS Measurements

Sample	$t < 20$ Å	20 Å $< t <$ 400 Å	$t >$ 400 Å
PLA-01	99.5%	0.3%	0.2%
PLA-02	99.8%	0.15%	0.05%
PLA-03	99.9%	0.05%	0.05%
PLA-04	99.8%	0.15%	0.05%

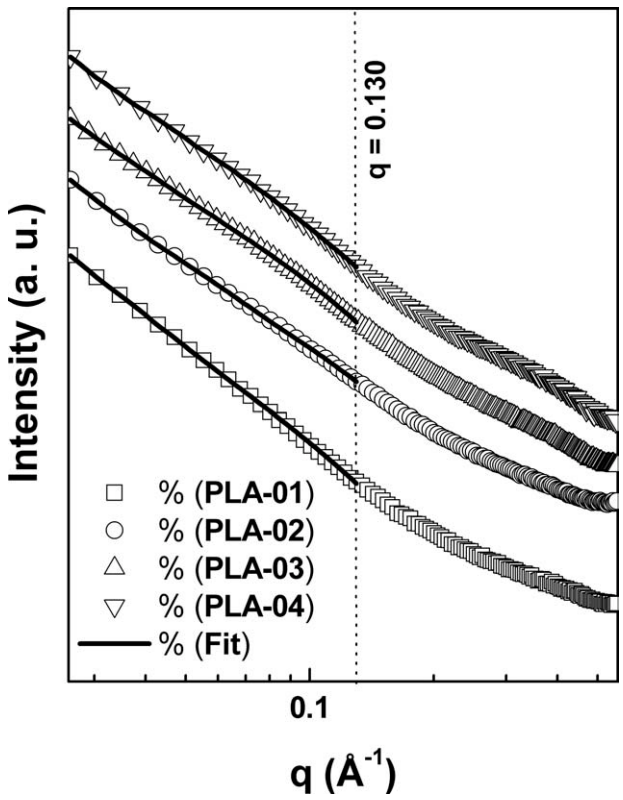

Figure 4 SAXS patterns of the PLA/clay nanocomposites and corresponding fits by using eq. (6).

exfoliated platelets seem to lead to a correlation bump around $q = 0.09$ Å^{-1} that increases its intensity with the increase of the clay content. This is illustrated by the increase of the parameter k, determined from the curves fitting, from 0.09 to 0.187 by increasing clay concentration from 3.6–13 wt %.

Conversion

There are many procedures for measuring the residual lactide concentration in PLA. Polarimetry, gel permeation chromatography, nuclear magnetic resonance, and simple gravimetric means after polymer precipitation are some of the methods documented in the literature.[21–31] Unfortunately, many of those analytical methods are not applicable for direct determination of monomer conversion in nanocomposites. For instance, our attempts to use ^{1}H-NMR for monitoring the conversion directly via integration of the methyl resonances of lactide and polylactide resulted in superimposed broad signals in the nanocomposites spectra, useless for any quantitative purpose. Aiming to overcome this problem we have decided to search for a simple and reliable method for determining the monomer conversion. Several studies discuss the use of Fourier transform infrared spectroscopy for lactide conversion analysis. Braun et al. have developed a rapid method for measuring lactide concentration in polylactide matrices using the lactide ring breathing mode peak at 935 cm^{-1}. They selected the asymmetric bending mode of methyl groups at 1454 cm^{-1} to normalize the lactide breathing signal and built a calibration curve using samples with well-defined composition of lactide and PLA. The method relies only on the lactide concentration in the sample and the clay content present in the nanocomposites does not exert any influence on the results. To our knowledge, this is the first time FTIR is employed for determining the lactide conversion in PLA/clay nanocomposites.

To employ the method established by Braun et al. a calibration curve was built using the 1454 and 935 cm^{-1} peak areas of defined blends of PLA and lactide (Table II).

As it can be seen in Figure 5, there is a linear relationship between the inversion of conversion and the peak area ratio for monomer conversions above 50%. Since the range of interest for high conversions usually involves lactide concentrations of 10% or less, the curve should be applicable for the nanocomposites prepared in this work. Figure 6 shows the infrared spectra for the PLA/clay nanocomposites.

The conversions calculated for the PLA/clay samples employing the FTIR method were determined to be no less than 94% for all PLA/clay samples within 3 h of reaction (Table III). Those are interesting results compared to the previously data reported by Paul et al. Even with no prior monomer swelling in the clay, the treatment with Tin(II) 2-ethyl-hexanoate seems to generate more active centers inside the organo-modified clay. That behavior might be explained by the formation of tin-alkoxide species through the eq. (7).

TABLE II
Calibration Curve Parameters Established with the Known Lactide/PLA Compositions

Blend composition		Conversion		Peak area		Peak area
Lac. (%)	PLA (%)	X	$1/X$	λ_1 (935 cm^{-1})	λ_2 (1454 cm^{-1})	ratio λ_1/λ_2 ($Z_{P/L}$)
5	95	0.95	1.05	0.276	11.753	0.023
10	90	0.90	1.11	0.118	1.975	0.060
20	80	0.80	1.25	0.236	1.848	0.128
30	70	0.70	1.43	1.336	5.835	0.229
50	50	0.50	2.00	7.336	14.253	0.515

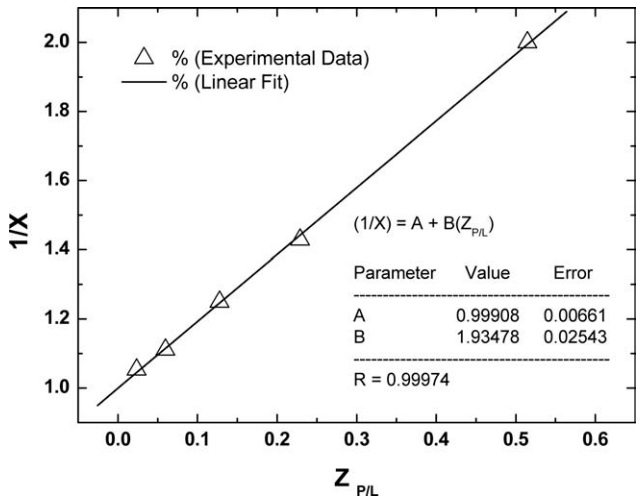

Figure 5 Inversion of conversion ($1/X$) plotted as a function of the peak area ratio ZP/L.

$$\mathrm{Sn(Oct)_2 + ROH \longrightarrow OctSnOR + OctH} \qquad (7)$$

The actual active site for lactide polymerization can be formed in reaction with H_2O, hydroxyl acids, alcohol or any coinitiator containing available hydroxyl groups.[23] After de formation of the Sn-OR bond, the subsequent monomer insertion propagation takes place. Many authors have stressed the relevance of coinitiators such alcohols in polymerization reactions with $Sn(Oct)_2$.[32–36] When purified $Sn(Oct)_2$ is used without any coinitiator purposely added, polymerization is very slow and shows the basic features of living polymerization: M_n increases linearly with conversion (no chain transfer changing the number of chains) and first-order kinetic plots are linear (no measurable termination). When a coinitiator is added the polymerizations are much faster and the relationship between M_n and conversion looses its linearity. That might explain why the pretreated clay seems to be more efficient compared to the direct mixture of $Sn(Oct)_2$ and the organo-modified clay in presence of molten lactide.

TABLE III
Calculated Parameters for the PLA/clay Nanocomposites from the Curve $1/X$ vs. $Z_{P/L}$

Sample	Peak area λ_1 (935 cm^{-1})	Peak area λ_2 (1454 cm^{-1})	Peak area ratio λ_1/λ_2 ($Z_{P/L}$)	Conversion X
PLA-01	0.380	20.488	53.915	0.969
PLA-02	0.438	16.161	36.897	0.950
PLA-03	0.256	12.069	47.144	0.945
PLA-04	0.352	14.769	41.957	0.957

Thermal properties

Figure 7 shows the DSC traces for the PLA/clay nanocomposites. The measurements were performed immediately after melting-quenching scans, so the samples have the same thermal history. In all curves it can be seen a steplike change around 58°C due to the T_g (glass transition temperature) of PLA for all samples. Table IV presents the data on the thermal transitions and degree of crystallinity obtained by DSC.

Although the glass transition temperature does not seem to be significantly affected by the presence of the clay in the polymer, the melting temperatures and the melting enthalpies (T_m and ΔH_m) are clearly shifted to lower values as the clay content increases. The decrease of the melting enthalpy at higher filler content could be related to the PLA chains length. Indeed, as the Cloisite® 30B loading in the nanocomposites increases, the concentration of hydroxyl

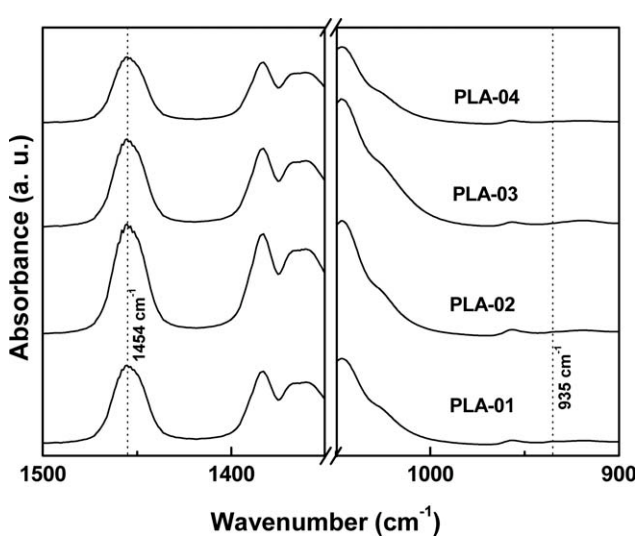

Figure 6 Selected spectral regions from 1500 to 1350 cm^{-1} and from 1050 to 900 cm^{-1} of the PLA/clay nanocomposites.

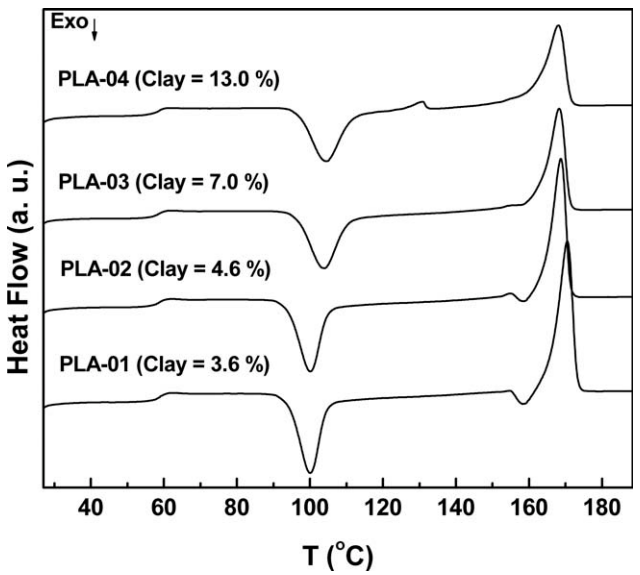

Figure 7 DSC scans of the PLA/clay nanocomposites.

TABLE IV
Thermal Properties of the PLA/Clay Nanocomposites

Parameters	PLA-01	PLA-02	PLA-03	PLA-04
Clay wt %	3.6	4.6	7.0	13.0
T_g (°C)	58.4	58.4	58.0	58.0
T_{hc} (°C) [ΔH_{hc} (J/g)]	100.2 [33.7]	100.0 [33.0]	103.7 [31.2]	104.4 [30.4]
T_{cc} (°C) [ΔH_{cc} (J/g)]	98.6 [30.0]	97.6 [22.9]	94.2 [5.8]	94.1 [1.9]
T_m (°C) [ΔH_m (J/g)]	170.4 [54.4]	168.7 [44.2]	168.2 [37.8]	168.9 [38.3] 129.5 [2.1]
$X_c = (\Delta H_m/\Delta H_m{}^0).100$	51.3	41.7	35.7	38.1

groups initiating the lactide polymerization increases in the same manner, leading to shorter PLA grafts, which need less thermal energy to melt. This effect on the thermal properties of nanocomposites has also been observed in a similar PLA/clay system.[3]

The influence of the clay can be also noted in the crystallization on heating temperature behavior (T_{hc}). From Table IV data it can be seen that the higher is the clay content in the nanocomposite, the higher the crystallization temperature is achieved. The effect of the clay particles on the crystallization on heating behavior in PLA nanocomposites seems to be controversial in the literature. While some authors reported that the increase of the clay content enhances the rate of crystallization others have considered that the clay has little nucleation effect because the crystallization temperature of the PLA matrix did not depend on the clay content.[37,38] Wu et al., studied the cold crystallization and kinetics of polylactide/clay nanocomposites.[39] According to their results the addition of very small amounts of clay (1–2 wt %) increased the crystallization rate evidently due to the nucleation effect, while further addition of clay impeded the crystallization on heating of the PLA matrix. The presence of clay resulted in a diffusion-controlled growth of nucleation of the PLA matrix, and the impeding effect of clay became gradually dominant with increasing loading levels especially in the case of high-rate nucleation. This statement is in agreement with the crystallization on cooling temperatures (T_{cc}) obtained from our DSC experiments.

CONCLUSIONS

Highly exfoliated polylactide/organo-modified montmorillonite nanocomposites were prepared with distinct clay content by using a catalyst based on an organo-clay treated with Sn(II) 2-ethyl-hexanoate. The FTIR spectra of the tin-clay indicate that the catalytic centers are fixed within the silicate galleries what can be considered an important condition for obtaining PLA/clay nanocomposites with high degree of exfoliation. From the quantitative FTIR method employed for the conversion determination we concluded that the supported catalyst reacts much faster than the previously reported clay/tin systems in the literature, reaching about 94% of conversion within 3 h of reaction with no previous monomer swelling step. The morphology study confirms the efficiency of the catalyst for the preparation of exfoliated PLA/clay nanocomposites through the absence of characteristic basal peak of the organo-modified clay in the X-ray diffraction patterns of the samples. The clay aggregates distribution determined from the SAXS curves showed that more than 99% of the clay fragments dispersed into the polylactide have thickness around 20 Å or less in all samples corroborating the X-ray diffraction information. The influence of the nano-sized clay fragments in the thermal properties of the nanocomposites can be clearly seen by the changes in the DSC scans. The shifts in the crystallization and melting temperatures with the increasing clay content suggest a diffusion-controlled growth of nucleation. Although the intercalative *in situ* polymerization is not well explored technique these results confirmed that it can be an efficient way to prepare PLA nanocomposites with high degree of exfoliation, which can be used for the manufacture of PLA masterbatches.

The authors would like to thank *Programa de Engenharia Metalúrgica e de Materiais - PEMM/COPPE/UFRJ* for the atomic absorption analyses and Prof. Emerson Oliveira da Silva for his help in the FTIR discussion.

References

1. Paul, M.-A.; Alexandre, M.; Degée, P.; Henrist, C.; Rulmont, A.Dubois, P. Polymer 2003, 44, 443.
2. Ray, S. S.; Yamada, K.; Okamoto, M.; Ueda, K. Polymer 2003, 44, 857.
3. Paul, M.-A.; Delcourt, C.; Alexandre, M.; Degée, P.; Monteverde, F.; Rulmont, A.; Dubois, P. Macrom Chem Phys 2005, 206, 484.
4. Urbanczyk, L.; Ngoundjo, F.; Alexandre, M.; Jérôme, C.; Detrembler, C.; Calberg, C. Eur Polym J 2009, 45, 643.
5. Bordes, P.; Pollet, E.; Avérous, L. Prog Polym Sci 2009, 34, 125.
6. Paul, M.-A.; Alexandre, M.; Degée, P.; Calberg, C.; Jérôme, R.; Dubois, P. Macromol Rapid Commun 2003, 24, 561.
7. Brügel, W. An Introduction to Infrared Spectroscopy, 2nd ed., Wiley: London and New York, 1962.

8. Braun, B.; Dorgan, J. R.; Dec, S. F. Macromolecules 2006, 39, 9302.
9. Sarasua, J. R.; Arraiza, A. L.; Balerdi, P.; Maiza, I. J Mater Sci 2005, 40, 1855.
10. Sarasua, J. R.; Prud'Homme, R. E.; Wisniewski, M.; Le Borgne, A.; Spasski, N. Macromolecules 1998, 31, 3895.
11. Lee, K. M.; Han, C. D. Macromolecules 2003, 36, 7165.
12. Madejová, J. Vibrational Spectroscopy 2003, 31, 1.
13. Kozak, M.; Domka, L. J Phys Solids 2003, 65, 441.
14. Mendioroz, S.; Pajares, J. A.; Benito, J.; Pesquera, C.; Gonzáles, F.; Blanco, C. Langmuir 1987, 3, 676.
15. Madejová, J.; Janek, M.; Komadel, P.; Herbert, H. J.; Moog, H. C. App Clay Sci 2002, 20, 255.
16. Pluta, M.; Jeszka, J. K.; Boiteux, G. Eur Polym J 2007, 43, 2819.
17. Porod, G. General Theory in Small Angle X-Ray Scattering. London: Academic Press, 1982.
18. Hanley H. J. M.; Muzny, D. D.; Butler, B. D. Langmuir 1997, 13, 5276.
19. Beaucage, G. J Appl Crystallography 1995, 28, 717.
20. Hajji, P.; David, L.; Gerard, J. F.; Pascault, J. P.; Vigier, G. J Polym Sci Part B Poly Phys 1999, 37, 3172.
21. Kowalski, A.; Libiszowski, J.; Duda, A.; Penczek, S. Macromolecules 2000, 331964.
22. Kowalski, A.; Duda, A.; Penczek, S. Macromolecules 1998, 31, 2114.
23. Kowalski, A.; Duda, A.; Penczek, S. Macromolecules 2000, 33, 7359.
24. Nijenhuis, A. J.; Grijpma D. W.; Pennings A. J. Macromolecules 1992, 25, 6419.
25. Li, S.; Girard, A.; Garreau, H.; Vert, M. Polym Degrad Stab 2001, 71, 61.
26. Stridsberg, K.; Albertsson, A.-C. J Polym Sci: Part A: Polym Chem 2000, 38, 1774.
27. Thakur, K. A. M.; Munson E. J.; Kean, R. T. Macromolecules 1997, 30, 2422.
28. Du, Y. J.; Lemstra, P. J.; Nijenhuis, A. J.; Van Aert, H. A. M.; Bastiaansen, C. Macromolecules 1995, 28, 2124.
29. Zhu, K. J.; Xiangzhou, L.; Shilin, Y. J Appl Polym Sci 1990, 39, 1.
30. Kricheldorf, H. R.; Damrau, D.-O. Macromol Chem Phys 1998, 199, 1747.
31. Kricheldorf, H. R.; Damrau, D.-O. Macromol Chem Phys 1997, 198, 1753.
32. Korhonen, H.; Helminen, A.; Seppälä, J. V. Polymer 2001, 42, 7541.
33. Kowalski, A.; Duda, A.; Penczek, S. Macromol Rapid Commun 1998, 19, 567.
34. Kowalski, A.; Duda, A.; Penczek, S. Macromolecules 2000, 33, 689.
35. Kricheldorf, H. R.; Kreiser-Saunders, I.; Stricker, A. Macromolecules 2000, 33, 702.
36. Duda, A.; Penczek, S.; Kowalski, A. Macromol Symp 2000, 153, 41.
37. Ray, S. S.; Yamada, K.; Okamoto, M.; Ogami, A.; Ueda, K. Chem Mater 2003, 15, 1456.
38. Ogata, N.; Jimenez, G.; Kawai, H.; Ogihara, T. J Polym Sci B: Polym Phys 1997, 35, 389.
39. Wu, D.; Wu, L.; Yu, L.; Xu, B.; Zhang, M. Polym Int 2009, 58, 430.